J|A|C|S ARTICLES

Published on Web 05/15/2009

Acid-Induced Amino Side-Chain Interactions and Secondary Structure of Solid Poly-L-lysine Probed by ^{15}N and ^{13}C Solid State NMR and *ab Initio* Model Calculations

Alexandra Dos,[‡] Volkmar Schimming,[‡] Monique Chan Huot,[‡] and Hans-Heinrich Limbach*,[‡]

Institut für Chemie und Biochemie, Takustrasse 3, Freie Universität Berlin, D-14195 Berlin, Germany

Received February 20, 2009; E-mail: limbach@chemie.fu-berlin.de

Abstract: The acid−base and base−base interactions of the ^{15}N-labeled side-chain amino groups of dry solid poly-L-lysine (PLL) and the consequences for the secondary structure have been studied using high-resolution solid state ^{15}N and ^{13}C CPMAS NMR spectroscopy. In a previous study we had shown that at acid/base ratios of 1 per amino group the halogen acids HI, HCl and HBr form PLL salts in the β-pleated sheet but not in the α-helical structure, whereas HF and various oxygen acids form 1:1 acid−base hydrogen-bonded complexes in both secondary structures. In the present study we performed NMR experiments at reduced acid/base ratios in order to elucidate whether also 1:2 and 1:3 acid−base complexes are formed under these conditions. Generally, the PLL samples containing HF, HBr, HCl, HI, CH_3COOH, H_3PO_4, H_2SO_4, or HNO_3 were obtained by lyophilization at different pH. For comparison, samples were also obtained by letting dry acid-free PLL interact with gaseous HCl. In a theoretical section we first study the probability of the different acid−base complexes as a function of the acid/base ratio and the equilibrium constants of the complex formation. Using this information, the ^{15}N NMR spectra of acid doped PLL obtained were analyzed and assigned. Indeed, evidence for the formation of 1:2 and 1:3 acid−base complexes at lower acid/base ratios could be obtained. Moreover, the salt structures of the halides of PLL are already destroyed at acid/base ratios of about 0.8. By contrast, when acid-free poly-L-lysine is exposed to HCl gas, a biexponential conversion of amino groups into ammonium groups is observed without formation of 1:2 and 1:3 complexes. ^{13}C NMR reveals that the β-pleated sheet environments of acid-free PLL react rapidly with HCl, whereas the α-helices first have to be converted in a slow reaction to β-pleated sheets before they can react. Interestingly, after partial doping with HCl, exposure to gaseous H_2O catalyzes the interconversion of the ammonium and amino groups into a mixture of 1:1, 1:2 and 1:3 complexes. Finally, the ^{15}N NMR assignments were assisted by DFT calculations on methylamine−acid model complexes.

Introduction

Poly-L-lysine (PLL, Scheme 1) is an important poly-amino acid which is used in numerous materials and drug delivery systems. In past years, in particular the secondary structures of PLL in aqueous solution and in the solid state have been of interest. X-ray diffraction studies of wet PLL × HCl[1] and of PLL × HBr fibers[2] revealed a β-pleated sheet structure, whereas wet PLL × H_3PO_4 crystallized as hexagonally arranged α-helices.[3] Removal of water leads in all cases to amorphous forms. Secondary structures have also been studied using various spectroscopic probes in aqueous solution.[4] The random coil is preferred at low pH. Raman optical activity (ROA)[5] studies showed regions of well-defined conformations including those corresponding to α-helix, β-pleated sheets and left-handed helix. At pH 9−11 a transformation to an α-helix was observed by ^{13}C NMR.[6] Heating the basic solution leads to formation of β-pleated sheet structures as revealed by ESR and NMR,[7] optical

Scheme 1. Chemical Structure of Poly-L-lysine Labeled with ^{15}N in the ε-Position (PLL)

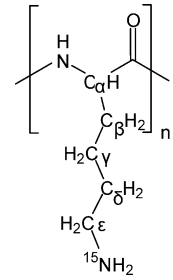

poly-L-lysine (PLL)

[‡] Chemie FU-Berlin.

(1) Shmueli, U.; Traub, W. *J. Mol. Biol.* **1965**, *12*, 205–214.
(2) Suwalsky, M.; Llanos, A. *Biopolymers* **1977**, *16*, 403–413.
(3) Cui, H.; Krikorian, V.; Thompson, J.; Nowak, A. P.; Deming, T. J.; Pochan, D. J. *Macromolecules* **2005**, *38*, 7371–7377.
(4) Ma, L.; Ahmed, Z.; Mikhonin, A. V.; Asher, S. A. *J. Phys. Chem. B* **2007**, *111*, 7675–7680.
(5) Wilson, G.; Hecht, L.; Barron, L. D. *J. Chem. Soc. Faraday Trans.* **1996**, *92*, 1503–1509.
(6) Saitô, H.; Smith, I. C. P. *Arch. Biochem. Biophys.* **1973**, *158*, 154–163.
(7) Perly, B.; Chevalier, Y.; Chachaty, C. *Macromolecules* **1981**, *14*, 969–975.

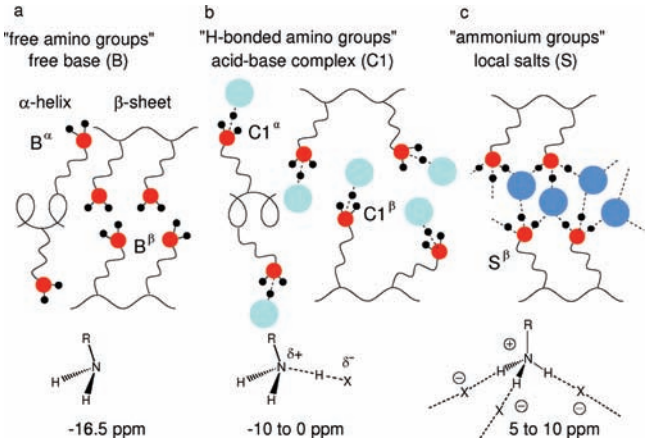

Figure 1. Hydrogen-bonded and protonation states (schematically) of dry solid PLL in the α-helical and the β-pleated sheet conformation according to ref 14. (a) Acid-free PLL exhibiting free basic amino groups B. (b) Acid−base complexes (C). C1-α and C1-β: 1:1 complexes in the α-helical and the β-pleated sheet conformation. (c) Salt structures (S).

rotatory dispersion (ORD) measurements[8] and Raman spectroscopy.[9] IR measurements showed that besides the temperature the formation of the β-sheet structure also depends on the chain length.[10]

However, because of the lack of spectroscopic probes, little is known about the protonation states and the mutual interactions of the amino side-chain groups. Typical for the protonated groups is an NH stretching band at 3030 cm^{-1} found by Rozenberg et al.[11] for dry solid PLL × HBr. In combination with other bands it was shown that PLL × HBr adopts a β-sheet structure when not all amino groups are protonated, but the random coil conformation which may be identical to the amorphous form is favored upon full protonation.

Hull et al.[12] have used the expected ^{15}N high-field shift of amines of about 10 ppm upon deprotonation[13] in order to measure the pK_a values of the PLL side chains in aqueous solution. Thus, the intrinsic ^{15}N chemical shifts measured at low and high pH refer to the hydrated alkylammonium and alkylamine side chains, whereas they represent averages at intermediate pH values.

Recently, some of us have shown that high-resolution solid state ^{15}N NMR CPMAS spectroscopy (CP = cross-polarization, MAS = magic angle spinning) carried out at high magnetic fields opens new possibilities to characterize the interaction of the amino groups of PLL with added acids.[14] It was shown that the ^{15}N chemical shifts of PLL × HX samples with one acid molecule per amino acid residue depend on the nature of the acid as illustrated in Figure 1. Whereas the free amino groups labeled as bases B resonate at −16.5 ppm with respect to external solid $^{15}NH_4Cl$, the halogen acids HCl, HBr and HI lead to values between 5 and 10 ppm, assigned to local salt structures S in agreement with the X-ray diffraction of the wet fibers,[2]

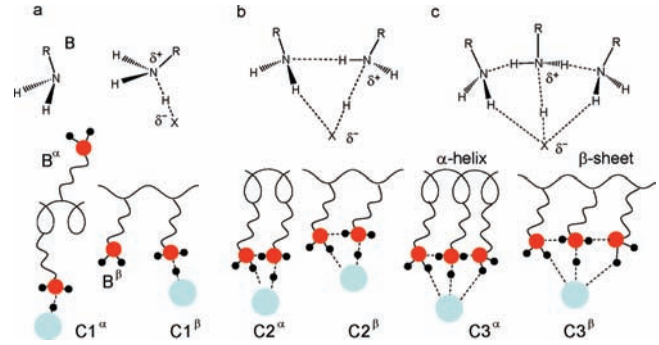

Figure 2. Potential hydrogen bonded and protonation states of dry solid PLL at acid/base ratios $X_{HX} < 1$. (a) Superposition of acid−base 1:1 complexes (C1) and free bases B; (b) 2:1 complexes C2; (b) 3:1 complexes C3.

where each amino nitrogen is coordinated to three halides and *vice versa*. However, the addition of HF and of other acids leads only to values between −10 and 0 ppm which were assigned to 1:1 hydrogen bonded complexes (C1). These complexes resemble those known for $NH_3 \times HX$ in the gas phase, which are molecular complexes;[15] strong electric fields arising from near dipoles are needed in order to form the NH_4Cl salt structure. Apparently, the polarity of dry solid PLL is so low that proton transfer to nitrogen does not occur unless halide salt structures can be formed in the β-sheet structures.

In this study, we have focused on the question how the amino groups react to a reduction of the acid concentration. Several scenarios are illustrated in Figure 2. Figure 2a refers simply to a superposition of free amino groups B and of 1:1 H-bonded complexes C1. As proton transfer is slow in the solid state, both environments should be detectable by solid state ^{15}N NMR. By contrast, in b and c of Figure 2 the free amino groups solvate the acid−base complexes leading to homoconjugated complexes C2 and C3 where two or three amino acid side chains share a proton. This internal solvation of ammonium by amino groups will assist H transfer from the acid to nitrogen. All three situations may be formed either starting from C1 (Figure 1b) or from local salt structures S (Figure 1c).

In order to obtain more information about this problem we have prepared solid poly-L-lysine enriched with ^{15}N in the ε-position of the side chains containing controlled amounts of various acids by lyophilization at different pHs in the presence of the appropriate acid counterions. In the case of HCl we also prepared a sample by letting react dry acid-free solid PLL with gaseous HCl. The state of the amino groups was then studied by high-resolution solid state ^{15}N CPMAS NMR. The samples were kept under argon gas in order to avoid the formation of carbamic acid in the solid state.[16] Whenever it seemed useful, we performed ^{13}C solid state NMR measurements in order to analyze the secondary structures according to the stratagem of Kricheldorf et al.[17] ^{13}C solid state NMR can also give information about the mobility of lysine side chains induced by hydration;[18−20] however, we did not yet study the effects of hydration of the ammonium groups, a task which we will perform in the near future. Furthermore, in order to obtain a feeling for the properties of C2 and C3 we have performed DFT

(8) Davidson, B.; Fasman, G. D. *Biochemistry* **1967**, *6*, 1616–1629.
(9) Painter, P. C.; Koenig, J. L. *Biopolymers* **1976**, *15*, 229–240.
(10) Jackson, M.; Haris, P. I.; Chapman, D. *Biochim. Biophys. Acta* **1989**, *998*, 75–79.
(11) Rozenberg, M.; Shoham, G. *Biophys. Chem.* **2007**, *125*, 166–171.
(12) Hull, W. E.; Kricheldorf, H. R.; Fehrle, M. *Biopolymers* **1978**, *17*, 2427–2443.
(13) Martin, G. J.; Martin M. L.; Gouesnard J.-P. *15N-NMR Spectroscopy*; Springer-Verlag: Berlin, Heidelberg, NY, 1981.
(14) Dos, A.; Schimming, V.; Tosoni, S.; Limbach, H. H. *J. Phys. Chem. B* **2008**, *112*, 15604–15615.
(15) Ramos, M.; Alkorta, I.; Elguero, J.; Golubev, N. S.; Denisov, G. S.; Benedict, H.; Limbach, H. H. *J. Phys. Chem. A.* **1997**, *101*, 9791–9800.
(16) Schimming, V.; Hoelger, C. G.; Buntkowsky, G.; Sack, I.; Fuhrhop, J. H.; Rocchetti, S.; Limbach, H. H. *J. Am. Chem. Soc.* **1999**, *121*, 4892–4893.
(17) Kricheldorf, H. R.; Müller, D. *Macromolecules* **1983**, *16*, 615–623.

calculations of the geometries and ^{15}N chemical shifts of these species in the presence of HCl and of acetic acid.

This report is organized as follows. In the Experimental Section are reported the details of (1) the sample synthesis and preparation, (2) the NMR studies and (3) the calculations. In the following Theoretical Section the association equilibria between free amino groups B and amino groups forming hydrogen bonds with acids are studied. This provides some general rules for the formation of the different species and the pH where the samples are lyophilized. Then we describe the results of the solid state NMR experiments on solid poly-L-lysine interacting with different acids. Finally, the results are discussed.

Experimental Section

NMR Samples. Poly-L-lysine hydrochloride (PLL × HCl) enriched with about 50% ^{15}N in the side chain amino groups was synthesized as described previously.[14] The molecular weight was 160000 ± 40000 Da, corresponding to 1000 ± 250 monomers in the polypeptide.[14]

pH measurements were carried out with a Hanna Instruments pH meter (HI9025), using a Mettler Toledo (Inlab 423), a Hanna Instruments (HI1332B) or a Hamilton Spintrode electrode. Before measurement the pH meter was calibrated using two of three buffer solutions (pH 4, pH 7, pH 10, Merck/Eurolab).

Liquid samples were prepared by dissolving about 5 mg of PLL × HCl in about 0.7 mL of water leading to 0.04 M solutions with respect to lysine monomers. The pH was adjusted with small quantities of HCl or NaOH in the same solvent. The samples with pH > 8 were frozen and warmed to room temperature only shortly before the NMR experiments in order to prevent gel formation.

Solid samples of PLL × HX were prepared by dialysis of PLL × HCl against dilute aqueous solutions of the desired acid. The solutions were then set to the desired pH by adding small quantities of a sodium hydroxide solution or of the desired acid. Finally, the samples were lyophilized. In the case of the acid- and ion-free sample an aqueous solution of PLL × HCl was desalted using an anion-exchange resin (Bio Rad AGI-X2, 200−400 mesh, OH^--form or Dowex 2 × 8−200, 100−200 mesh, OH^- -form prepared from the Cl^- form). This leads to an increase of the pH to about 12. Then the sample was lyophilized and dried.

During the operations described above contact with air was minimized in order to avoid carbamate formation of PLL. It occurs in water around pH 10 as well as in the dry solid state in acid-free dry PLL.[14,16] Therefore, all solutions as well as the bidistilled water, were degassed *in vacuo* and were consequently flushed with argon.

The lyophilized samples were transferred into rotors and consecutively dried further inside the uncapped rotor at room temperature *in vacuo* at pressure below 10^{-6} mbar. On average the samples were kept at this pressure for 16−20 h and then flushed with dry argon. The rotors were closed with Teflon sealing caps and measured by NMR.

In order to study the interaction of PLL with gaseous HCl, a PLL sample lyophilized at pH 12 was placed in an NMR rotor, dried *in vacuo* at 298 K and 10^{-6} mbar for 16−20 h, and then exposed for different amounts of time to gaseous HCl (1 bar). Between each exposure a ^{15}N CPMAS NMR spectrum was taken.

NMR Spectroscopy. All solid-state measurements were carried out on a Varian Infinity Plus 600 spectrometer at a ^{15}N resonance frequency of 60.8 MHz and a ^{13}C resonance frequency of 150.88 MHz. All measurements were performed at ambient temperature. Spinning speeds between 5 and 10 kHz were used. The ^{13}C NMR spectra were calibrated to TSP ($Si(CH_3)_3-CD_2-CD_2-COO-Na^+$). The ^{15}N solid state NMR spectra were referenced to solid NH_4Cl using glycine (100% ^{15}N- and ^{13}C-enriched) as an intermediate reference.

The ^{15}N chemical shifts measured recently for aqueous solution[14] were referenced to solid $^{15}NH_4Cl$ as described before[21] using neat nitromethane as intermediate external reference. The ^{15}N chemical shift of the latter had been established with respect to solid $^{15}NH_4Cl$ by Hayashi et al.[22] who found that $\delta(CH_3{}^{15}NO_2, \text{liq.}) = \delta(^{15}NH_4Cl, \text{solid}) - 341.168$ ppm. Note that an often used alternative reference, liquid ammonia, resonates at −38.16 ppm with respect to solid $^{15}NH_4Cl$, i.e. at −379.33 ppm with respect to neat nitromethane.[23]

Ab Initio and Chemical Shift Calculations. The calculations of methyl amine with different counterions in the gas phase were performed at the B3LYP/6-31 g(d,p) level[24] using Gaussian 03[25] in a similar way as described previously. This program also allowed us to calculate the isotropic and anisotropic GIAO nuclear magnetic shielding values of all nuclei, but only the ^{15}N values were analyzed.

Theoretical Section. In this section we derive and discuss the occurrence of the different amino side-chain species illustrated in Figure 2 as a function of pH. We assume that in the dry solid state the relative distribution of the different species can be described in terms of the equilibria between C1 ≡ XHB, C2 ≡ XHB_2, and C3 ≡ XHB_3,

$$\mathrm{C1} + \mathrm{B} \overset{K_1}{\rightleftharpoons} \mathrm{C2},\ K_1 = \frac{c_{\mathrm{C2}}}{c_{\mathrm{C1}} c_{\mathrm{B}}} \tag{1}$$

and

$$\mathrm{C2} + \mathrm{B} \overset{K_2}{\rightleftharpoons} \mathrm{C3},\ K_2 = \frac{c_{\mathrm{C3}}}{c_{\mathrm{C2}} c_{\mathrm{B}}} \tag{2}$$

characterized by the equilibrium constants K_1 and K_2, where c_i is the concentration of species i. The total concentration of the amino side chains is given by

$$C_{\mathrm{B}} = c_{\mathrm{B}} + c_{\mathrm{C1}} + 2c_{\mathrm{C2}} + 3c_{\mathrm{C3}} \tag{3}$$

and the acid concentration by

$$C_{\mathrm{HX}} = c_{\mathrm{C1}} + c_{\mathrm{C2}} + c_{\mathrm{C3}} \tag{4}$$

where it is assumed that all acid molecules are bound to an amino group. This condition will be fulfilled in good approximation when $C_{\mathrm{HX}} < C_{\mathrm{B}}$. Defining the mole fractions $x_i = c_i/C_{\mathrm{B}}$ we can rewrite eqs 1 and 2 as

$$C_{\mathrm{B}} K_1 = \frac{x_{\mathrm{C2}}}{x_{\mathrm{C1}} x_{\mathrm{B}}},\ C_{\mathrm{B}} K_2 = \frac{x_{\mathrm{C3}}}{x_{\mathrm{C2}} x_{\mathrm{B}}} \tag{5}$$

As C_{B} is a constant for solid PLL it can be incorporated into the equilibrium constants, *i.e.* be removed from the left sides of eq 5. Let us define the acid base ratio as

$$X_{\mathrm{HX}} = \frac{C_{\mathrm{HX}}}{C_{\mathrm{B}}} = x_{\mathrm{C1}} + x_{\mathrm{C2}} + x_{\mathrm{C3}} \tag{6}$$

(18) Swanson, S. D.; Bryant, R. C. *Biopolymers* **1991**, *31*, 967–973.
(19) Krushelnitsky, A.; Faizullin, D.; Reichert, D. *Biopolymers* **2004**, *73*, 1–15.
(20) Zanotti, J. M.; Bellissent-Funel, M. C.; Parello, J. *Biophys. J.* **1999**, *76*, 2390–2411.
(21) (a) Sharif, S.; Denisov, G. S.; Toney, M. D.; Limbach, H. H. *J. Am. Chem. Soc.* **2007**, *129*, 6313–6327. (b) Sharif, S.; Schagen, D.; Toney, M. D.; Limbach, H. H. *J. Am. Chem. Soc.* **2007**, *129*, 4440–4455. (c) Sharif, S.; Chan Huot, M.; Tolstoy, P. M.; Toney, M. D.; Jonsson, K. H. M.; Limbach, H. H. *J. Phys. Chem. B* **2007**, *111*, 3869–3876. (d) Sharif, S.; Denisov, G. S.; Toney, M. D.; Limbach, H. H. *J. Am. Chem. Soc.* **2006**, *128*, 3375–3387.
(22) Hayashi, S.; Hayamizu, K. *Bull. Chem. Soc. Jpn.* **1991**, *64*, 688–690.
(23) Harris, R. K. *Pure Appl. Chem.* **1998**, *70*, 117–142.
(24) Becke, A. D. *J. Chem. Phys.* **1993**, *98*, 5648.
(25) Frisch, M. J.; et al. *Gaussian 98*, revision A.11; Gaussian, Inc.: Pittsburgh PA, 2001 For the full ref see Supporting Information.

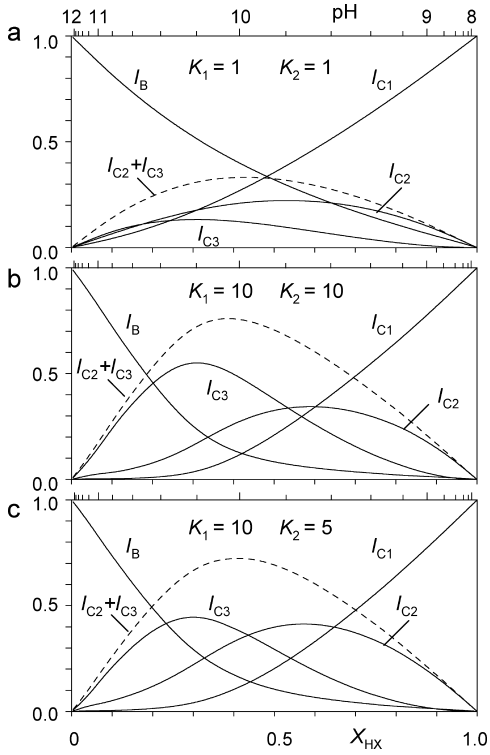

Figure 3. Distribution of hydrogen-bonded acid/base 1:1 complexes (C1) of type XHB, 1:2 complexes (C2) of type XHB_2, and 1:3 complexes (C3) of type XHB_3 calculated using a combination of eqs 1 to 9 as a function of the total acid/base ratio $X_{HX} = C_{HX}/C_B$. K_1 and K_2 represent the equilibrium constants defined in eqs 1 and 2 and C_{AH} and C_B, the total acid and base concentrations. For further discussion see text.

This ratio in the lyophilized dry PLL samples is equal to the pH-dependent degree of protonation of the amino groups in solution given by[14]

$$X_{BH+} = X_{HX} = \frac{1}{1 + 10^{pH-pK_a}}, \quad pK_a = 9.85 \tag{7}$$

where it had been assumed that the pK_a values of the amino groups are independent of each other, i.e. where anticooperativity effects were neglected.

By combination of the above eqs we obtain

$$K_2 x_{C2}^2 + x_{C2}(1 + K_2(1 - 3X_{HX} + 2x_{C1})) - X_{HX} + x_{C1} = 0 \tag{8}$$

with

$$\begin{aligned} I_{C2} &= 2x_{C2} = \frac{2K_1 x_{C1}(1 - 3X_{HX} + 2x_{C1})}{1 - K_1 x_{C1}}, \\ I_{C3} &= 3x_{C3} = 3(X_{HX} - x_{C1} - x_{C2}), \\ I_B &= x_B = 1 - x_{C1} - 2x_{C2} - 3x_{C3} \end{aligned} \tag{9}$$

The quantities I_i stand for the probability to find a nitrogen atom in species i. The I_i can be better compared to the relative ^{15}N signal intensities than the mole fractions x_i when the different nitrogen sites of i are not resolved.

It is difficult to obtain analytical expressions for x_i and hence of I_i as a function of the total acid/base ratio $X_{HX}$with the equilibrium constants as parameters. Therefore, the desired relations were computed numerically for arbitrary values of K_1 and of K_2. The results are depicted in Figure 3. For convenience, the abscissa is labeled not only by the acid/base ratio X_{HX} but also by the pH of lyophilization, calculated according to eq 7. The solid lines refer to the total expected relative nitrogen signal intensities I_i, and the dashed line to the sum of the intensities of C2 and C3.

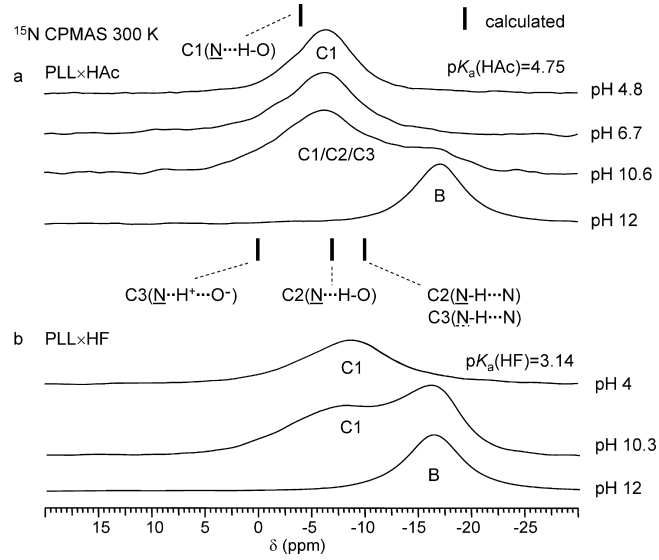

Figure 4. ^{15}N CPMAS spectra (60.8 MHz) of dry lyophilized PLL-$^{15}N_\varepsilon$ doped with different amounts of (a) acetic acid and (b) HF. The samples were obtained by lyophilization at different pH in the presence of the corresponding sodium salts and subsequent drying *in vacuo*.

When we set both equilibrium constants to unity we obtain the graph depicted in Figure 3a. At pH values below the pK_a value of 9.85, complex C1 and above this value the free base B dominate. The maximum value of I_{C2} occurs around pH 9.8, and that of I_{C3}, around pH 10.4. This result is not much altered when the equilibrium constants are changed. In Figure 3b we set $K = K_2 = 10$. Now, C3 dominates above pH 10. This can be rationalized as follows. For infinite equilibrium constants, $X_{HX} = 0.1$, it is easy to show that $I_{C3} \approx 0.3$, whereas at $X_{HX} = 0.9$, I_{C2} adopts only a value of 0.2, which explains the different curves for C2 and C3. We note that this result does not substantially change if one reduces the value of K_2 as illustrated in Figure 3c.

We obtain the following conclusions for solid state ^{15}N NMR of the amino groups of PLL. When lyophilization is performed at pH 10.4 and above, and if a ^{15}N signal is observed which differs from those of C1 and of B, this signal has to be attributed to a mixture of C2 and C3, with a preference for the latter.

Results

pH Dependence of $^{15}N_\varepsilon$-Poly-L-lysine in Aqueous Solution. The ^{15}N NMR spectra of $^{15}N_\varepsilon$-poly-L-lysine in aqueous solution at 283 K as a function of pH have been reported previously.[14] The limiting chemical shift of the protonated amino group was found to be $\delta_{NH3+} = -6.1$ ppm at low pH. The value of the deprotonated amino group was found to be $\delta_{NH2} = -13.94$ ppm. The Henderson−Hasselbalch plot (eq 7) gave a single pK_a value of 9.85 ± 0.20 for all amino groups as already mentioned in the previous section. Equation 7 was then used to estimate the acid fraction of the lyophilized PLL samples from the pH value where the lyophilization took place. This approach is not precise as it is conceivable that (i) in water the pK_a value of a given amino group might be influenced by the protonation state of neighboring amino groups (anticooperative effect) and (ii) that the acid fraction X_{HX} might change in the last stages of the lyophilization process.

Dependence of the $^{15}N_\varepsilon$ Chemical Shifts of Dry Lyophilized PLL as a Function of the Acid Concentration. HF and Oxygen Acids. In Figures 4 and 5 are depicted the ^{15}N CPMAS NMR spectra of dry samples of PLL × HF, PLL × CH_3COOH,

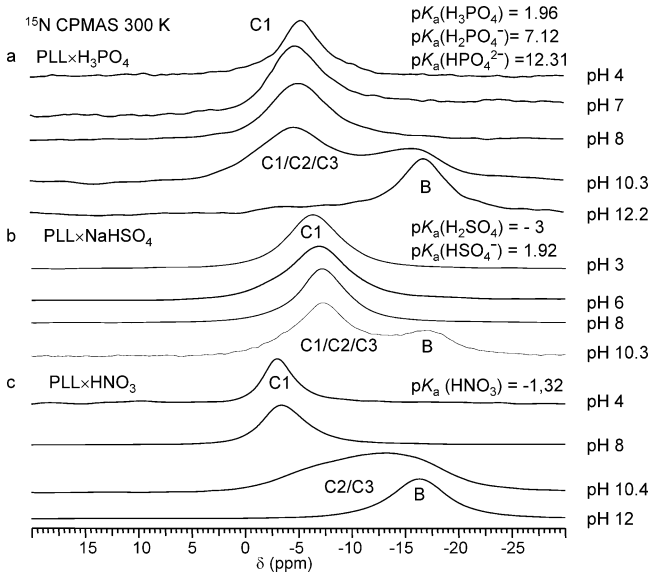

Figure 5. ^{15}N CPMAS spectra (60.8 MHz) of dry lyophilized PLL-$^{15}N_\varepsilon$ doped with different amounts of (a) $H_3PO_4/H_2NaPO_4/HNa_2PO_4$, (b) H_2SO_4 /$NaHSO_4$, (c) HNO_3. For further description see text.

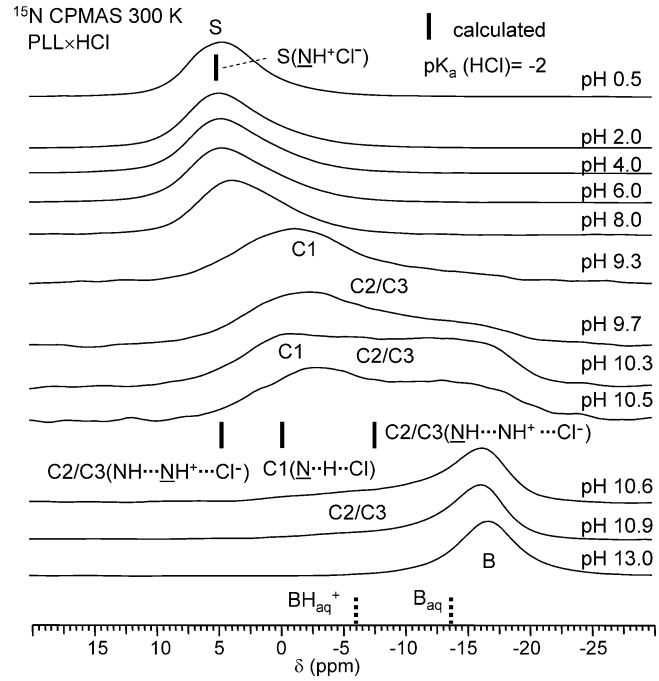

Figure 6. ^{15}N CPMAS spectra (60.8 MHz) of dry lyophilized PLL-$^{15}N_\varepsilon$ doped with different amounts of HCl. For further description see text.

PLL × H_3PO_4, PLL × H_2SO_4, and PLL × HNO_3 prepared at different acid/base ratios X_{HX} by lyophilization at different pH as described in the Experimental Section.

We have added in Figures 4 and 5 the pK_a values of the acids employed. They indicate the protonation state of the acid during the lyophilization process. This is especially important in the case of H_2SO_4 and of H_3PO_4 where the active acids may correspond to the partially deprotonated species.

At $X_{HX} = 0$, i.e. lyophilization at pH 12, in all cases sharp signals for the free amino groups B are observed at −16.5 ppm. By contrast, at pH values below 8, i.e. $X_{HX} = 1$, the above acids form in the lyophilized dry solid state hydrogen bonded complexes C1 with the amino groups, as argued previously.[14] The chemical shifts range from −9 ppm in the case of PLL × HF to −3 ppm in the case of PLL × HNO_3. Calculations on methylamine−acid complexes indicated that these changes arise from an increase of the HX distances. However, even in PLL × HNO_3, it was argued that H is still located closer to $X = O$ than to N.[14]

At intermediate pH values, especially around pH 10.5, interesting spectral features are observed for all acids, as depicted in Figures 4 and 5. Besides the signal of B and the signals assigned to C1 a new broad signal is observed between −5 and −10 ppm. This signal is well distinguished from signal B. The difference to C1 and B is best pronounced in the case of HNO_3 as acid (Figure 5c), because its C1 signal is shifted downfield as compared to the corresponding signal of the other acids. The different behavior of HF and acetic acid is striking. In the HF case, the signals can be interpreted without the appearance of C2/C3, whereas this signal is clearly observed for acetic acid, although it is barely shifted as compared to the C1 complex. However, as predicted by Figure 3, when the equilibrium constants of C2 and C3 formation are small, only C1 and B can be observed (Figure 4b). By contrast, if these constants are large, the C2/C3 signal dominates, and B remains small (Figure 4a).

C2 and C3 contain different nitrogen atoms of the type NHNHX and NHNHX. In order to obtain a feeling how much their chemical shifts vary we have performed chemical shielding calculations of methylamine−acid complexes whose results are described later. In Figure 4 we have visualized the calculated and extrapolated ^{15}N chemical shifts of methylamine-acetic acid complexes C1 to C3 as vertical bars. Note that C1 and C2 were found to be molecular complexes in the gas phase whereas C3 exhibited a zwitterionic character. The chemical shift changes between the different nitrogen sites are, however, not large. Thus, formation of C2 and C3 can explain the observed signal broadening when samples are lyophilized between pH 10 and 11, although a distinction between both types of complexes was not possible.

We conclude that in the presence of the oxygen acids containing more than one oxygen the formation of C2/C3 is favored, whereas it does not seem to occur in the case of HF.

Halogen Acids Forming Local Salt Structures with PLL. The ^{15}N CPMAS spectra of PLL × HI, PLL × HBr and of PLL × HCl lyophilized at different pH are depicted in Figures 6 and 7. Again, the vertical bars represent the results of the chemical shielding calculations described below. Below pH 8 only little changes are observed as the acid/base ratio is $X_{HX} = 1$. Broad lines are observed for the three systems, where PLL × HCl is centered around 5 ppm, PLL × HBr around 7 and PLL × HI around 9 ppm. These signals were assigned previously[14] to local salt structures S as illustrated in Figure 1, where all NH bond lengths are around 1 Å corresponding to alkyl ammonium groups. Ideally, each group interacts with three halide anions and *vice versa*, but local disorder can lead to a distribution of local structures and hence ^{15}N chemical shifts. The large downfield shifts as compared to the oxygen acids arise from anisotropic shielding contributions of the halides which increase with the size of their electronic system, i.e. from chlorine to iodine.[14]

When the acid/base ratio is decreased, interesting features are observed. In the case of PLL × HCl a sudden high-field shift to about −2 ppm is observed when the acid/base ratio is reduced to about 0.8 by lyophilization at pH 9.3. This line is compatible with the calculated chemical shift of C1; apparently

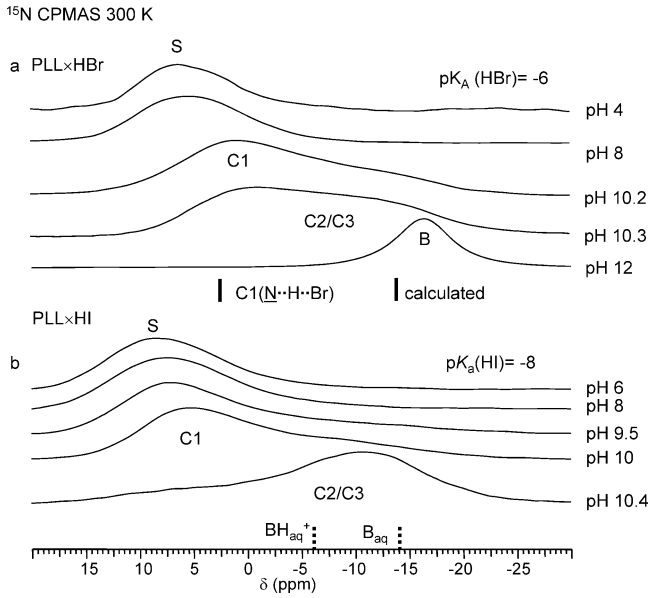

Figure 7. ^{15}N CPMAS spectra (60.8 MHz) of dry lyophilized PLL-$^{15}N_{\varepsilon}$ doped with different amounts of (a) HBr and (b) HI. For further description see text.

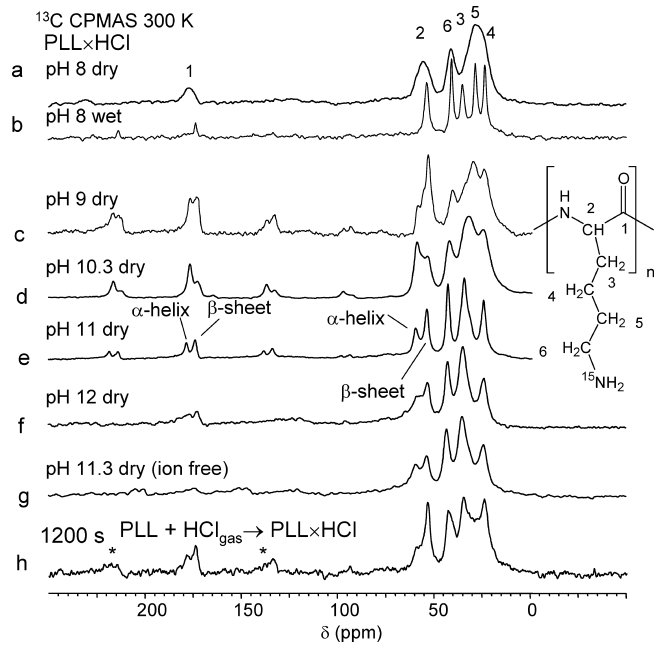

Figure 8. ^{13}C CPMAS spectra of solid PLL. (a) PLL × HCl lyophilized at pH 8 and dried *in vacuo*. (b) Same sample after exposure for 12 h to air saturated with water at 298 K. (c) to (f) PLL lyophilized in the presence of chloride at pH 9, 10.3, 11, and 12 and dried subsequently *in vacuo*. (g) Dry ion-free PLL. (h) Sample of dry ion-free PLL after exposure to dry gaseous HCl for 1200 s. For further description see text.

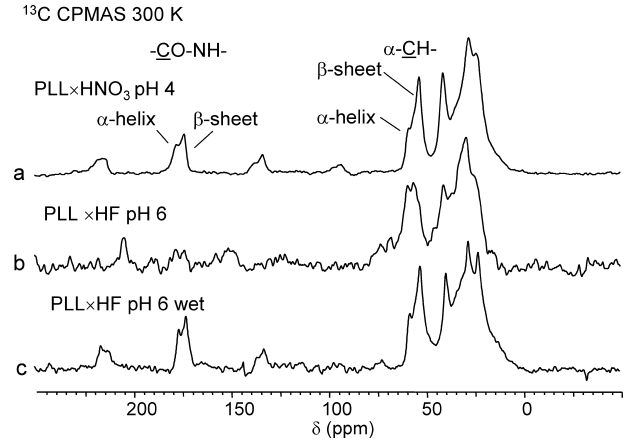

Figure 9. ^{13}C CPMAS spectra of (a) PLL × HNO_3 and lyophilized at pH 4, (b) PLL × HF lyophilized at pH 6, and (c) same sample after exposure to air at 298 K saturated with water.

this strongly hydrogen bonded complex is formed when the local salt structure is disassembled. In addition, a smaller broad signal around −7 ppm is observed, which we assign again to C2/C3; as described later, these complexes exhibit a zwitterionic structure. The line assigned to C1 decreases and those assigned to C2/C3 increase when the acid/base ratio is reduced; however, signal B typical for free amino groups only appears when lyophilization is carried out above pH 10. Similar features are observed for PLL × HI and PLL × HBr. As expected, the signal assigned to C1 is shifted downfield when going from chlorine to iodine.

^{13}C NMR of Dry Lyophilized PLL as a Function of the Acid Concentration. In order to know whether there is an interplay between the hydrogen bond and protonation states and the secondary structures of PLL we performed ^{13}C CPMAS NMR experiments on various PLL samples where we changed the acids and their concentrations. As was described by Kricheldorf et al.,[17] the carbonyl groups of the α-helix and of the *β*-pleated sheets resonate at 176 and 172 ppm, and the corresponding α-CH carbons of the side chain at 58 and 52 ppm.

Figure 8a depicts a spectrum of a dry PLL × HCl sample obtained by lyophilization at pH 8. When the sample was exposed to humid air we obtained the spectrum shown in Figure 8b. In the dry sample the above-mentioned peaks are broad, but wettening gives rise to sharp bands typical for *β*-pleated sheets. These environments were already assigned to local salt structures S. These findings confirm that dry samples of PLL × HCl are amorphous whereas wet samples exhibit a high degree of crystallinity.[2] Similar results are obtained by lyophilization at lower pH values.

By contrast, lyophilization in the presence of chloride at higher pH values up to 12 produces a mixture of α-helices and of the *β*-pleated sheets as illustrated in Figure 8c to 8f. This is the region where ^{15}N NMR indicates the presence of hydrogen bonded complexes, where C1 is converted gradually into C2 and C3 as the acid/base ratio is reduced, and eventually to the free base B. A similar mixture of both α-helices and of the *β*-pleated sheets is also formed in the absence of acid (Figure 8 g). Thus, we conclude that hydrogen-bonded complexes C1 to C3 and the free base can be formed with both secondary structures.

Finally, we have included in Figure 8h a spectrum which was obtained from an acid-free dry sample by exposure to gaseous HCl for 1200 s. This spectrum will be discussed in the next section where this experiment is described in more detail.

Figure 9 depicts ^{13}C CPMAS spectra of PLL doped with HNO_3 and HF. Both exhibit signals for a mixture of both α-helices and of the *β*-pleated sheets; again, this is typical for hydrogen-bonded complexes which confirms the interpretation of the ^{15}N NMR spectra.

Reaction of Dry Solid PLL with Gaseous HCl. In order to elucidate whether the way of preparation has an influence on the acid−base structures of PLL we prepared two dry ion- and acid-free PLL samples as described in the Experimental Section.

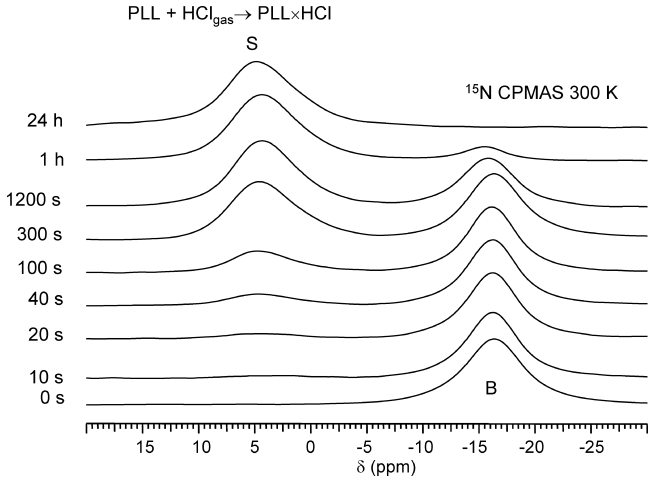

Figure 10. ^{15}N CPMAS spectra (60.8 MHz) of dry ion-free PLL-$^{15}N_\varepsilon$ after exposure to dry gaseous HCl for different reaction times.

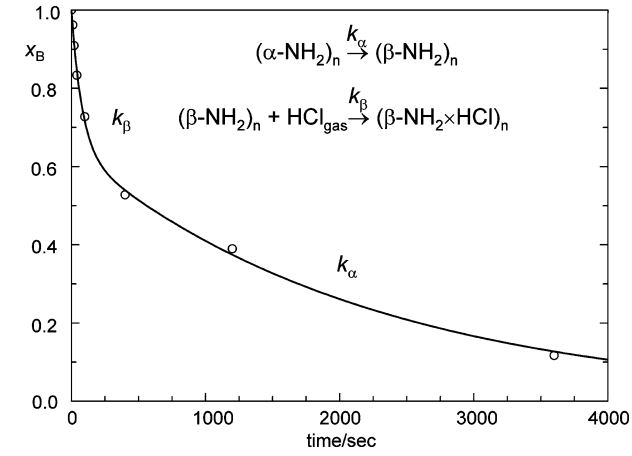

Figure 11. Fraction of the free-base signal B in Figure 10 as a function of the reaction time. The solid line was calculated by nonlinear least-squares fitting to eq 10. The fast decay characterized by the rate constant k_β is assigned to the protonation of the β-pleated sheets. The slow decay described by k_α is assigned to the slow interconversion of the α-helical regions into β-pleated sheets.

Sample no. 1 was exposed to 1 bar of dry gaseous HCl for a total of 1200 s, and sample no. 2 for a total of 24 h, interrupted for short intervals in which ^{15}N CPMAS NMR spectra were taken as illustrated in Figure 10.

Initially, only the ^{15}N signal of the free base B was observed at −16.5 ppm, but after less than 1 min exposure to HCl the expected low-field signal S at 5 ppm appeared. Eventually, signal S increased, and B disappeared. The final spectrum was identical with the upper spectrum in Figure 6 obtained by lyophilization at low pH values. However, no signals come up at intermediate reaction times in the region expected for C1 and C2, C3, in contrast to lyophilization at pH values between 9 and 11 (Figure 6).

From the areas under the signals in Figure 10 we calculated the mole fraction x_B of the free base B and plotted this quantity in Figure 11 as a function of time. Clearly, a biexponential behavior with a fast and a slow component is observed. The solid line was calculated using

$$x_B = A_\alpha \exp(-k_\alpha t) + A_\beta \exp(-k_\beta t),$$
$$A_\alpha = 0.64, k_\alpha = 4.51\times10^{-4}\ s^{-1}, A_\beta = 0.36, k_\beta = 0.0127\ s^{-1} \quad (10)$$

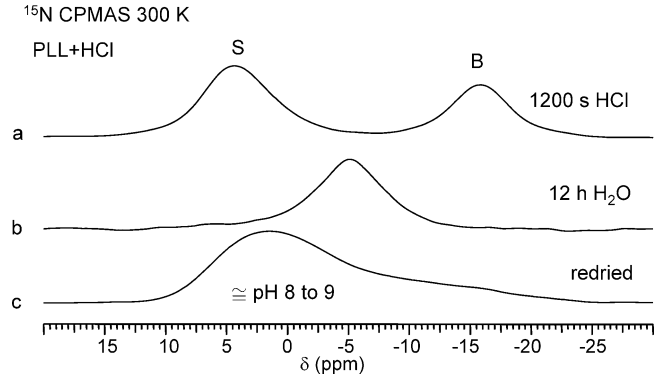

Figure 12. ^{15}N CPMAS spectra of dry PLL (a) exposed for 1200 s to gaseous HCl. (b) Same sample after exposure for 12 h to air saturated with water for 12 h at 298 K. (c) After redrying *in vacuo*.

where x_B represents the fraction of the free amino group signal B, A_α and A_β the amplitudes, and k_α and k_β pseudo-first-order rate constants. These parameters were determined by a nonlinear least-squares fitting procedure. At 1200 s the fast signal conversion is complete and the slow one to about 40%.

At this point, we come back to the ^{13}C NMR spectrum of Figure 8h which was taken 1200 s exposure to gaseous HCl. As compared to the spectrum in Figure 8g taken before HCl exposure, the signals of the α-helices have been reduced to about 50% of their original values, and those of β-pleated sheets have been increased.

Therefore, we identify the amplitudes A_α and A_β in eq 10 with the fraction of α-helices and of β-pleated sheets in the acid-free dry solid PLL sample. The β-pleated sheets domains can react rapidly with gaseous HCl - characterized by k_β - to form local salt structures S which are partially disordered as indicated by the broad ^{13}C and ^{15}N signals. Amino groups in α-helices can not react with HCl as they can not easily form local salt structures. However, they interconvert slowly - characterized by the rate constant k_α - to β-pleated sheet domains which then react rapidly with HCl.

After having been exposed for 1200 s to gaseous HCl the ^{15}N spectra indicate a free base fraction of 0.4 and hence an acid/base ratio of 0.6. According to the Henderson−Hasselbalch plot[14] of PLL, such an acid content can be produced by lyophilization in the presence of chloride around pH 9.5. According to Figure 6, such a sample will exhibit a broad signal centered at −2 ppm, in contrast to the sample no. 1 doped for 1200 s via the gas phase.

In order to understand this difference we exposed this sample to humid argon at room temperature saturated with water for 12 h. In Figure 12 the spectrum obtained after exposure (Figure 12b) is compared to the spectrum before exposure (Figure 12a). Apparently, water entered the sample and leads afterward to a coalescence of the two signals around −5 ppm. When we redried the sample *in vacuo* we obtained a spectrum (Figure 12c) which corresponds to the spectra obtained by lyophilization around pH 9 (Figure 6). Thus, the sample composition obtained after 1200 s exposure to gaseous HCl with a superposition of domains exhibiting β-sheets with local alkyl ammonium salt structures and α-helical domains with nonprotonated amino groups is not thermodynamically stable; water increases the local mobility and "catalyzes", therefore, the formation of C1 to C3 complexes which are thermodynamically more stable at acid/base ratios of about 0.6 than the salt structures S. Only when the acid/base ratio increases to about 1 are the β-sheets with local alkyl ammonium salt structures the thermodynamically stable species.

Table 1. Calculated Interatomic Distances, ^{15}N Chemical Shielding and Anisotropy Values of Methylamine−Acid Clusters[a]

−	$-BH^+$	$-B_2H^+$	$-B_3H^+$	−B × HCl	$-B_2$ × HCl	$-B_3$ × HCl	−B × HAc	$-B_2$ × HAc	$-B_3$ × HAc
r(N1H1X)	1.026	−	−	1.553	1.113	1.067	1.706	1.619	1.142
r(N1H1X)	−	−	−	1.400	1.815	2.006	1.016	1.038	1.416
r(N1H1X)	−	−	−	2.952	2.904	2.983	2.703	2.654	2.544
r(N3H7X)	−	−	1.020	−	−	1.029	−	−	1.032
r(N3H7X)	−	−	−	−	−	2.459	−	−	2.164
r(N3H7X)	−	−	−	−	−	3.386	−	−	3.076
r(N2H5X)		1.511	1.020		1.027	1.029		1.023	1.024
r(N2H5X)	−	−	−	−	2.540	2.462	−	2.019	1.897
r(N2H5X)	−	−	−	−	3.429	3.389	−	3.025	2.913
r(N1H2N2)	−	1.162	1.082	−	1.058	1.055	−	1.035	1.053
r(N1H2N2)	−	1.511	1.725	−	1.838	1.489	−	1.984	1.835
r(N1H2N2)		2.673	2.806	−	2.818	2.889	−	2.984	2.842
r(N1H3N3)	−	−	1.082	−	−	1.055	−	−	1.036
r(N1H3N3)	−	−	1.725	−	−	1.852	−	−	2.036
r(N1H3N3)		−	2.807	−	−	2.820	−	−	2.914
σ(N1)	235.22	227.85	223.98	224.61	219.79	217.78	229.50	233.01	222.82
$\Delta\sigma$(N1)	7.33	7.84	6.37	14.69	23.05	16.35	36.16	29.38	16.27
δ(N1)	−8.3	−2.6	0.4	−0.1	3.7	5.2	−3.9	−6.6	1.3
σ(N2)	−	233.03	237.13	−	232.94	234.22	−	239.34	236.03
$\Delta\sigma$(N2)	−	15.68	18.49	−	32.29	33.20	−	31.89	32.79
δ(N2)	−	−6.6	−9.8	−	−6.6	−7.6	−	−11.5	−11.3
σ(N3)	−	−	237.19	−	−	234.21	−	−	239.05
$\Delta\sigma$(N3)	−	−	18.40	−	−	33.41	−	−	34.86
δ(N3)	−	−	−9.9	−	−	−7.6	−	−	−9.0

[a] B = CH_3-NH_2. σ isotropic and $\Delta\sigma$ anisotropic chemical shielding values in ppm, distances *r* in Å. δ chemical shift extrapolated using eq 14.

Calculated Hydrogen Bond Geometries of Methyl Amine−HCl Complexes of the Type C2 and C3. In order to assist the spectral assignment of the complexes C2 and C3 we have calculated the optimized equilibrium geometries of the corresponding methylamine−acid complexes $B_2 \times HX$ and $B_3 \times HX$, with HX = H^+, HCl and acetic acid. The structures of the corresponding complexes BHX of the C1 type had been reported previously together with calculations of C1 complexes involving other acids and of halide salt structures S.[14] In addition to the geometries, also the isotropic and anisotropic ^{15}N chemical shielding values were calculated. All results are assembled in Table 1, and the optimized geometries, in Figure 13.

Discussion

Using solid state ^{15}N NMR we have shown that the ^{15}N chemical shifts of the side chain N_ε amino groups of dry lyophilized PLL can probe a number of different hydrogen bonded and protonation states, which depend on the acid−base ratio $X_{XH} = C_{XH}/C_B$. Here, C_{XH} represents the concentration of the added acid molecules and C_B the concentration of the amino groups. Moreover, the protonation and hydrogen bonded states influence the secondary structures. In the following, we will first discuss the structures formed at intermediate acid/base ratios, a discussion which is assisted by the results of DFT calculations performed on methylamine−acid clusters. In the second part, we will address the relation between hydrogen bond and protonation states with the secondary structure, as well as with the method of doping.

Structures of Methylamine−Acid Model Complexes. As models for the side chains of PLL in the dry solid state at acid/base ratios smaller than unity we have calculated the properties of the isolated 2:1 and 3:1 methylamine × HCl complexes C2 and C3 depicted in Figure 13. These studies complete those published previously of various 1:1 complexes C1 as well as of halide salt clusters S.[14] The calculations show that the molecular conformation, the hydrogen bond geometries and protonation states depend on the number of methylamine and acid molecules in the clusters. The complexes with H^+ as acid exhibit trans-structures for the methyl groups, whereas cis-structures are obtained for the other acids. The NHN hydrogen bonds of the 2:1 complexes are not symmetric, i.e. the proton is located nearer one of the two atoms. The potential energy curves of the proton motions were not explored further.

The proton in the 1:1 complex with HCl is located closer to Cl than to N, but is shifted to nitrogen in the 2:1 and 3:1 complexes. By contrast, acetic acid is not strong enough in order to transfer its proton to two base molecules. For that three base molecules and a very special conformation is needed as illustrated in Figure 13c.

Hydrogen Bond Correlation Analysis. At this stage, it is useful to compare the calculated hydrogen bond geometries of methylamine−acid complexes of the C2 and C3 type with those calculated previously for the C1 type.[14] For that purpose we use the well established hydrogen bond correlation analysis. Let $r_1 = r_{BH}$ and $r_2 = r_{HX}$ be the two heavy atom-hydrogen distances of a hydrogen bond BHX. It is then convenient to define the proton and the heavy atom coordinates

$$q_1 = 1/2(r_1 - r_2) \text{ and } q_2 = r_1 + r_2 \qquad (11)$$

For a linear hydrogen bond q_2 is equal to the heavy atom distance and the proton coordinate q_1 the distance of H from the H-bond center. One can associate to both bonds valence bond orders given by[26]

$$p_1 = \exp\{-(r_1 - r_1^o)/b_1\} \text{ and } p_2 = \exp\{-(r_2 - r_2^o)/b_2\} \qquad (12)$$

r_1^o and r_2^o represent the equilibrium distances in the fictive free diatomic units AH and HX, and b_1 and b_2 describe bond order decays with increasing bond distances. As the valence of hydrogen is unity, $p_1 + p_2 = 1$, both distances r_1 and r_2 depend on each other. Thus, it is possible to express r_1 as a function of r_2, or q_1 as a function of q_2. The validity of this equation has

(26) (a) Pauling, L. *J. Am. Chem. Soc.* **1947**, *69*, 542–553. (b) Brown, I. D. *Acta Crystallogr.* **1992**, *B48*, 553–572. (c) Bürgi, H. B.; Dunitz, J. D. *Acc. Chem. Res.* **1983**, *16*, 153–161.

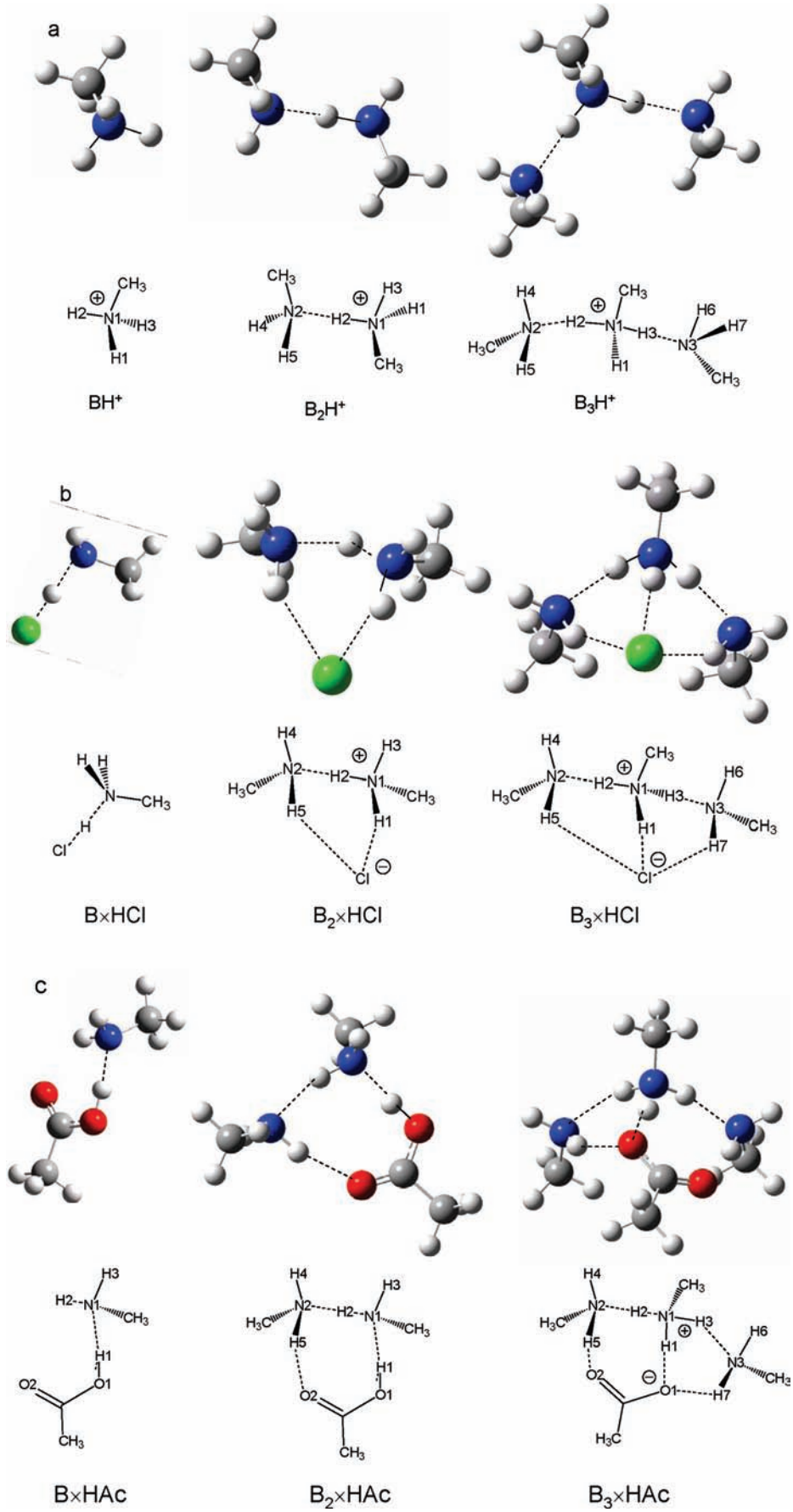

Figure 13. Equilibrium structures of methylamine−acid 1:1, 2:1 and 3:1 clusters calculated using DFT methods. Acid: (a) H^+, (b) HCl, (c) acetic acid. For further description see text.

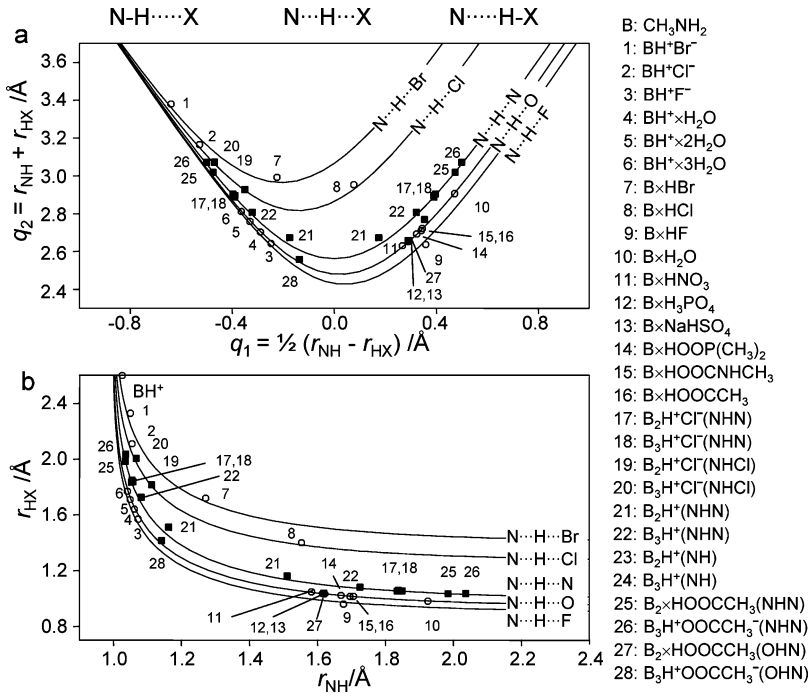

Figure 14. Hydrogen bond correlation of calculated equilibrium structures of methylammonium halide salt structures and of methylamine−acid complexes. (a) Heavy atom coordinate q_2 as a function of the hydrogen bond coordinate q_1. (b) r_{HX} as a function of r_{NH}. The solid correlation lines and the data points 1−12 were taken from ref 14.

been demonstrated in a number of cases.[21,27,28] An empirical correction for quantum zero-point vibrational effects (QZPVE) was introduced recently which needs to be taken into account when discussing H/D isotope effects on hydrogen bond geometries.[29,30]

In Figure 14a are plotted the calculated equilibrium coordinates q_1 as a function of q_2, and in Figure 14b the corresponding distances r_{HX} as a function of r_{NH}. The equations and parameters used to calculate the different correlation curves represented by the solid lines have been reported recently[14] and are based on previous work.[15,31] The open circles stem from 1:1 complexes of the C1 type and from salt structures.[14] All data points are well located on the correlation curves. New are the data points calculated in this study for the clusters of the C2 and C3 types. The new data points are symbolized by solid squares. They are also well located on the NHN, NHO and NHCl correlation curves. Figure 14 confirms that simple correlation lines without correction for quantum zero-point vibrational effects (QZPVE) can describe the data calculated for the equilibrium geometries of hydrogen-bonded systems.[21,27,28,30,32]

This hydrogen bond correlation analysis allows us also to analyze the calculated isotropic chemical shielding constants σ_N of the amino nitrogen atoms interacting with selected acids as a function of the distances r_{NH} (Table 1). The open circles in Figure 15a refer to data for the C1 complexes of methylamine as well as to methylammonium bromide and chloride (entries 1 and 2) reported previously.[14] The filled squares refer to equilibrium geometries of the methylammonium clusters of Figure 13. The dashed correlation curves were calculated as described previously[14,33] using the equation[27,,30]

$$\sigma_N = \sigma(\underline{N}HX) = \sigma(\underline{N}H)°p_{NH} + \sigma(\underline{N})°p_{HX} - 4\sigma*(\underline{N}HX)p_{NH}p_{HX}^m \quad (13)$$

$\sigma(\underline{N}H)°$ represents the shielding constant of isolated protonated methylamine $CH_3NH_3^+$, set to 235 ppm and $\sigma(\underline{N})° = 244$ ppm the value of the unprotonated isolated methylamine CH_3NH_2.[14] These values are independent of the acid. Thus, $\sigma(\underline{N}H)° - \sigma(\underline{N})°$ represents the protonation shift, and these values were kept constant for all correlation lines in Figure 15. $\sigma*(\underline{N}HX)$ stands for the decrease of the shielding in the strongest hydrogen bond. The parameter m influences the shape of the correlation curve. The values used to calculate the dashed lines in Figure 15a were assembled in Table 3 of ref 14 and do not need to be repeated here. The new solid NHN correlation curve was calculated using the values $\sigma*(\underline{N}HX) = 11.2$ ppm and $m = 0.6$.

Figure 15a shows that the calculated ^{15}N shielding constants of the acid−base complexes depend in a typical way on the distance r_{NH} as illustrated by the dashed line. The scattering of the data is a sign that also other structural features influence the shielding constants, for example multiple hydrogen bond contacts of the amino groups with multiple acceptor sites in the acid residues.

Qualitatively, the correlation curves indicate that the chemical shielding of free methylamine is reduced when it forms a

(27) Benedict, H.; Shenderovich, I. G.; Malkina, O. L.; Malkin, V. G.; Denisov, G. S.; Golubev, N. S.; Limbach, H. H. *J. Am. Chem. Soc.* **2000**, *122*, 1979–1988.
(28) Shenderovich, I. G.; Tolstoy, P. M.; Golubev, N. S.; Smirnov, S. N.; Denisov, G. S.; Limbach, H. H. *J. Am. Chem. Soc.* **2003**, *125*, 11710–11720.
(29) Limbach, H. H.; Pietrzak, M.; Benedict, H.; Tolstoy, P. M.; Golubev, N. S.; Denisov, G. S. *J. Mol. Struct.* **2004**, *706*, 115–119.
(30) Limbach, H. H.; Pietrzak, M.; Sharif, S.; Tolstoy, P. M.; Shenderovich, I. G.; Smirnov, S. N.; Golubev, N. S.; Denisov, G. S. *Chem.-Eur. J.* **2004**, *10*, 5195–5204.
(31) Limbach, H. H.; Denisov, G. S.; Golubev, N. S. Hydrogen Bond Isotope Effects Studied by NMR. In *Isotope Effects in the Biological and Chemical Sciences*; Kohen, A., Limbach, H. H., Eds.; Taylor & Francis: Boca Raton FL, 2005; Chapter 7, pp 193−230.
(32) Lopez, J. M.; Männle, F.; Wawer, I.; Buntkowsky, G.; Limbach, H. H. *Phys. Chem. Chem. Phys.* **2007**, *9*, 4498–4513.

(33) In eq 5 of ref 14 the last term on the right side should be negative. This typo has now been corrected in eq 13.

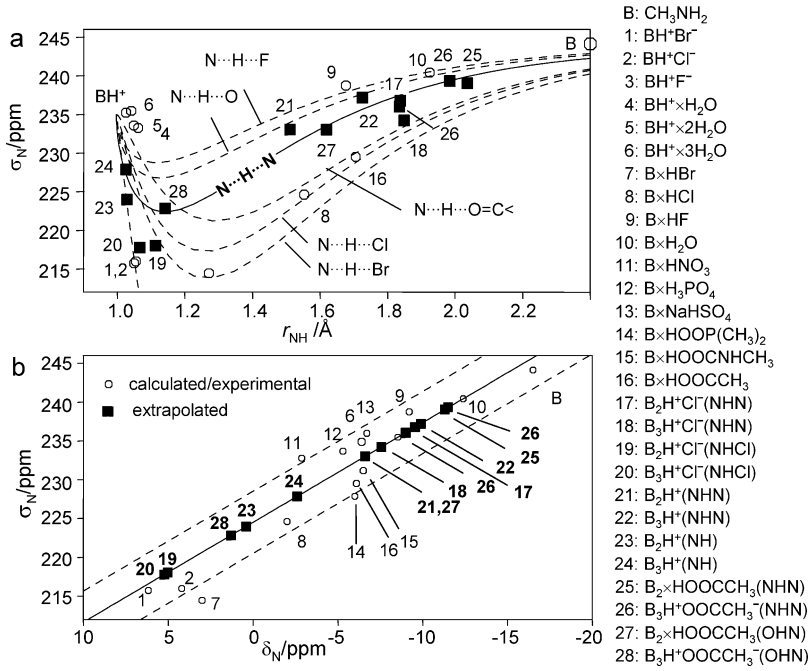

Figure 15. Calculated ^{15}N chemical shielding constants of methylammonium halides and of methylamine−acid complexes as a function of (a) the calculated r_{NH} values and (b) of the experimental ^{15}N chemical shifts of PLL interacting with the same acids. With exception of the NHN correlation line, the dashed curves and the data points 1 to 16 were taken from ref 14 New data points are 17 to 28. The new NHN correlation line was calculated using eq 13, a value of $\sigma^*(\underline{N}HN) = 11.2$ ppm and $m = 0.6$, the values of $\sigma(\underline{N})^\circ = 244$ ppm and $\sigma(\underline{N}H)^\circ = 235$ ppm were assumed to be the same for all correlation curves.

hydrogen bond with a proton donor. σ_N goes through a minimum when the hydrogen bond compression is largest, i.e. when q_2 goes through a minimum and H is located in the hydrogen bond center. σ_N then increases again when H is completely transferred to nitrogen. The main difference between the dashed correlation lines in Figure 15a arises from the deshielding term $\sigma^*(\underline{N}HX)$ in the strong hydrogen bond regime. This term is similar for F, aliphatic N and aliphatic O, but increases with the size of the electronic system of the bridge atom X of the acid, e.g. when going from chlorine to iodine. A further deshielding occurs when the number of coordinated halogen anions is increased to three, as in the methylammonium halide salts.[14] An additional deshielding is also observed for C1 complexes of acetic acid with methylamine when H is shifted artificially from O to N.[14] Whereas in the initial state a single H-bond is formed, two H-bonds between methylammonium and acetate are formed in the product. The neighboring effect of the carboxylate groups induces then an additional deshielding.

Let us now discuss the new data points calculated for the higher clusters C2 and C3, where HX = H^+, HCl and acetic acid. The shieldings of the external nitrogen atoms involved only in NHN bonds are well described by the solid correlation line, and reflect their hydrogen bond geometries. The shieldings of the nitrogen atoms interacting with the acids are, however, quite different. In the case of HX = H^+ the shielding is somewhat smaller than of free methylammonium, reflecting the influence of the neighboring amino groups. In the case of HCl the corresponding nitrogen atom feels the presence of the neighboring chloride and exhibits, therefore, a substantial deshielding. In the C3 complex with acetate the central nitrogen is involved in a strong OHN hydrogen bond and, therefore, deshielded because of the neighboring carboxylate. On the other hand, in the C2 complex H is located on oxygen, and the deshielding is smaller.

As discussed previously,[14] the calculated chemical shielding constants of the isolated complexes correlate well with those found for the acid−base complexes in PLL as illustrated in Figure 15b. The open circles refer mostly to the C1 complexes reported previously, where the solid correlation curve was expressed by the eq 14:

$$\sigma_N = -1.285 \times \delta_N + 224.5 \text{ ppm} \qquad (14)$$

Here, we have added the data points 7 and 8 which we have taken from the spectra of PLL × HCl and PLL × HBr after lyophilization between pH 9.3 and 10.3 (Figures 6 and 7). Within the margin of error, these data points are well located on the correlation curve.

In the next stage, we calculated estimates of the ^{15}N chemical shifts of the C2 and C3 complexes of PLL × X, HX = H^+, HCl and acetic acid by placing the calculated shielding constants on the solid correlation curve as depicted in Figure 15b. Thus, we predict chemical shifts between +4 and −10 ppm for these kinds of complexes. Taking into account that these hydrogen bonds are very polarizable leading to a distribution of hydrogen bond geometries, it becomes clear that C2 and C3 will resonate in the same region as the 1:1 complexes C1. This explains the finding in Figures 4 and 5 that the ^{15}N signals exhibit only little shifts when the acid/base ratio is reduced, although the nature of the complexes is changed from C1 to C2 and C3. By contrast, major changes are observed for the halide salts, which first form C1 complexes and then C2 and C3 complexes when the acid/base ratio is reduced.

We note that ^{15}N chemical shifts between 0 and −5 ppm have been observed recently[34] in solids exhibiting homoconjugated cations of the type $[R(CH_3)_2N\cdot\cdot H\cdot\cdot N(CH_3)_2R]^+$. This result

(34) Yaghmaei, S.; Khodagholian, S.; Kaiser, J. M.; Tham, F. S.; Mueller, L. J.; Morton, T. H. *J. Am. Chem. Soc.* **2008**, *130*, 7836–7838.

Scheme 2. (a) Doping of Acid-Free PLL with Gaseous HCl;[a] (b) Same Product Is Obtained by Lyophilization below pH 8 and Drying *in vacuo*; (c) Lyophilization above pH 8 Produces Hydrogen-Bonded 1:1, 1:2 and 1:3 Complexes C in both α-Helical Domains and β-Pleated Sheets. (d) Solid Mixture of Free Base B in α-Helical Domains and a Salt Structure S-β Is Not Stable but Converted by Humidity into a Mixture of H-Bonded Complexes C in Both Forms

a $[B^{\alpha}]_{solid} + HCl_{gas} \xrightarrow{k_{\alpha}} [B^{\beta}]_{solid} + HCl_{gas} \xrightarrow{k_{\beta}} [S^{\beta}]_{solid}$

b $[B^{\alpha/\beta}]_{aq} \xrightarrow{Cl^-,\ pH < 8} \xrightarrow{-H_2O} [S^{\beta}]_{solid}$

c $[B^{\alpha/\beta}]_{aq} \xrightarrow{Cl^-,\ pH > 8} \xrightarrow{-H_2O} [C^{\alpha/\beta}]_{solid}$

d $[B^{\alpha}/S^{\beta}]_{solid\ mixture} \xrightarrow{+H_2O_{gas}} \xrightarrow{-H_2O} [C^{\alpha/\beta}]_{solid}$

[a] Only β-pleated sheets can form salt structures S-β. α-Helical domains must first interconvert into β-pleated sheets before the doping is complete.

is in agreement with our findings of −5 to −10 ppm for C2 and C3 complexes as replacement of H in the ammonium cation by methyl groups leads to downfield shifts of 5 to 10 ppm. An example for this shift is the value of about +5 ppm for PLL hydrochloride with respect to ammonium chloride in Figure 6.

Secondary Structures, Hydrogen Bond and Protonation States of N_ε Amino Groups of Dry Solid PLL. In the experiments and calculations described above we have provided evidence that the amino side chains of dry PLL form 2:1 and 3:1 clusters with acids HX at low acid/amino group ratios. Depending on the acid and the cluster size, the acid shifts the proton more or less toward nitrogen. However, we suspected that cluster formation may be feasible only in special PLL conformations. As we also anticipated that molecular rearrangements are slow in dry solid PLL, we followed the incorporation of gaseous HCl into dry acid- and ion-free PLL by solid state ^{15}N NMR. The results of our studies are summarized in Scheme 2.

Dry solid acid-free PLL consists of a mixture of domains exhibiting an α-helical and a β-pleated sheet structure, labeled as $[B\text{-}\alpha/\beta]_{solid}$. When this solid is treated with HCl gas, only the β-pleated sheets $[B\text{-}\beta]_{solid}$ react with the acid to form local salt structures $[S\text{-}\beta]_{solid}$ within a time scale of minutes. This reaction is too slow to be explained in terms of HCl penetration of the solid or of proton transfer as rate-limiting steps. Therefore, the formation of salt structures requires probably side-chain motions which are slow in the absence of water. On the other hand, α-helical parts $[B\text{-}\alpha]_{solid}$ seem not to react directly with HCl. ^{13}C CPMAS NMR tells us that they need first to be converted into β-pleated sheets which then react with HCl (Figure 8h). This leads to the observed biexponential time dependence of the reaction with HCl (Figure 11). At the end, all amino groups are protonated, and the entire sample is converted into dry $[S\text{-}\beta]_{solid}$.

According to solid state ^{15}N and ^{13}C NMR, this state is also reached by lyophilization at pH values below 8 and extensive vacuum drying. It gives rise to broad signals and is consistent with the finding of an amorphous state when water is removed.[2] An ordered crystalline structure is only formed in the wet material, as indicated by ^{13}C CPMAS NMR (Figure 8) and X-ray crystallography.[2]

Whereas the interconversion of the secondary structures of the dry solids takes place in the hour time scale, the presence of water catalyzes this transformation. This was demonstrated with a dry sample partially doped with gaseous HCl, consisting of a mixture of the acid-free domains $[B\text{-}\alpha/\beta]_{solid}$ and of salt structures $[S\text{-}\beta]_{solid}$ (Figure 12a). When this sample was exposed to water vapor, ^{15}N NMR indicated an increased proton mobility (Figure 12b), and after water removal the sample was converted into a mixture of hydrogen-bonded C1 to C3 complexes, existing as α-helices and β-sheets (Figure 12c). This state is also reached by lyophilization between pH 8 and 9 and is, therefore, thermodynamically more stable than separate salt domains $[S\text{-}\beta]_{solid}$ and free-base domains $[B\text{-}\alpha/\beta]_{solid}$.

Conclusions

Our solid state NMR studies of dry solid poly-L-lysine (PLL) interacting with various acids, combined with DFT calculations on methylamine−acid complexes lead to the following conclusions. First, ^{15}N CPMAS is a very powerful tool for the study of the acid−base behavior of lysine side-chain amino groups as the relation between ^{15}N chemical shifts and protonation states has been studied both in our previous[14] and in the current study. When PLL is lyophilized and dried, the interaction of the side-chain amino groups with added acids changes its nature as compared to aqueous solution. In the latter a fast pH-dependent proton transfer equilibrium exists between the hydrated protonated and deprotonated ammonium/amino groups characterized in approximation by a single pK_a value (9.85) for all amino groups. By contrast, the pK_a concept in the dry solid state breaks down where proton transfer is quenched. Oxygen acids and HF only form hydrogen-bonded 1:1 complexes of the type C1 (Figure 1) in which H is located somewhere between nitrogen and the heavy atom of the acid. Nonprotonated amino groups try to solvate the amino/ammonium groups interacting with the added acid, by forming 2:1 or 3:1 complexes of the types C2 and C3 (Figure 2), giving rise to broad bands between −5 and −10 ppm (ref solid NH_4Cl). These new bands were best visualized in the case of HNO_3 as acid (Figure 5c) after lyophilization at pH 10.4. On the other hand, HCl, HBr and also HI[14] form salt structures S with PLL, where each ammonium group is interacting with three halides and *vice versa*. However, these salt structures are destroyed when the acid/base ratio is reduced, leading also to a superposition of complexes C1, C2 and C3. Moreover, these salt structures can only be formed in the β-pleated sheet conformation. This was demonstrated by an experiment in which dry acid-free PLL existing as a mixture of α-helical and β-sheet conformations was exposed to gaseous HCl. ^{13}C CPMAS NMR indicated a salt formation within minutes only of the β-pleated sheets (Figures 8h, 10 and 11); by contrast, α-helical conformations need to be first converted into sheet conformations which lasts several hours in the absence of water. At intermediate reaction stages the ammonium groups of the β-sheet salt structures and of the nonprotonated amino groups of the α-helical structures are in slow exchange within the NMR time scale. Probably, they form well-separated domains. However, exposure to humid air induced a fast exchange of both environments within the NMR time scale (Figure 12), and reorganization of the secondary structure as the initial superposition of ammonium and amino groups is not thermodynamically stable: after drying the spectra had changed, leading to the formation of C1, C2, and C3 complexes, a result which is also obtained by lyophilization at pH 8 to 9 (Figure 12).

These results demonstrate the connection between function and secondary structure in poly-L-lysine: a special acid−base interaction of the side-chain amino groups requires a special secondary conformation. The effects of hydration on the

acid−base interactions of PLL observed in Figure 12 are intriguing. They are in agreement with the finding that lysine side-chain motions are quenched in the absence of water.[20] Therefore, we have started to study the effects of hydration on the acid−base interactions of PLL. The results will be reported in a subsequent paper.

Acknowledgment. This work has been supported by the Deutsche Forschungsgemeinschaft and the Fonds der Chemischen Industrie, Frankfurt. We thank Prof. Dr. J. H. Fuhrhop, FU Berlin, and Dr. Sergio Tosoni, Humboldt Universität zu Berlin, for interesting discussions.

Supporting Information Available: Full ref 25. This material is available free of charge via the Internet at http://pubs.acs.org.

JA901082A